Inorg. Chem. **2009**, *48*, 1519−1523

Synthesis, Characterization, and Properties of Organically Templated Lanthanide Oxalatophosphates with a Three-Dimensional Honeycomb Structure: $(H_4APPIP)[Ln_3(C_2O_4)_{5.5}(H_2PO_4)_2]\cdot 5H_2O$ (Ln = Er−Lu, APPIP = 1,4-Bis(3-aminopropyl)piperazine)

Chih-Min Wang,[†,‡] Yi-Ying Wu,[†] Chia-Hung Hou,[§] Chii-Chang Chen,[§] and Kwang-Hwa Lii*[,†,‡]

Department of Chemistry, National Central University, Jhongli, Taiwan 320, ROC, Institute of Chemistry, Academia Sinica, Nankang, Taipei, Taiwan 115, ROC, and Department of Optics and Photonics, National Central University, Jhongli, Taiwan 320, ROC

Received September 23, 2008

Four isostructural organically templated lanthanide oxalatophosphates, $(H_4APPIP)[Ln_3(C_2O_4)_{5.5}(H_2PO_4)_2]\cdot 5H_2O$ (Ln = Er−Lu and APPIP = 1,4-bis(3-aminopropyl)piperazine), have been synthesized under hydrothermal conditions and characterized by single-crystal and powder X-ray diffraction. Their structures contain LnO_8 trigonal dodecahedra linked by three bis-bidentate oxalates to form layers in the (102) plane, which are connected by dihydrogen phosphate and bis-monodentate oxalate ligands to form a 3D framework. The charge-compensating tetraprotonated 1,4-bis-(3-aminopropyl)piperazinium cations and lattice water molecules are located in the 12-membered ring straight channels. They are the first examples of organically templated lanthanide oxalatophosphates. The thermal stability, guest desorption−sorption properties, variable-temperature in situ powder X-ray diffraction, magnetic susceptibility, and photoluminescence spectrum of the Er compound and catalytic activity of the Yb compound for the Biginelli reaction have also been studied.

Introduction

A large number of open-framework metal phosphates have been synthesized in the presence of organic amine templates because of their interesting structural chemistry and potential applications.[1] Recently, many research activities have focused on the synthesis of hybrid frameworks by incorporating organic ligands into the structures of metal phosphates. Among the large number of carboxylate compounds, the oxalate moiety, $C_2O_4^{2-}$, was found to be a good candidate and has been successfully incorporated into phosphate frameworks with transition metals and main group elements.[2] For example, the metal oxalatophosphates, $(H_3TREN)[M_2(C_2O_4)_{2.5}(HPO_4)]\cdot 3H_2O$ (M = Mn and Fe, TREN = tris(2-aminoethyl)amine), contain macroanionic planar sheets of the formula $[M_2(C_2O_4)_{2.5}(HPO_4)]^{3-}$ with the templating organic ammonium cations between adjacent sheets.[2g] Within a sheet, there are 12-membered pores made from six MO_6 octahedra, one phosphate, and five oxalate units. The structure motif is reminiscent of the honeycomb networks of bimetallic transition-metal oxalates of the general formula $[A^+][MM'(ox)_3]$, where A^+ is a templating inorganic or organic cation and M and M′ are divalent and trivalent transition-metal ions, respectively.[3] These compounds have been extensively researched because of their interesting structural chemistry and magnetic properties. In these 2D honeycomb networks, each six-coordinate transition-metal ion is linked to three others via bis-bidentate oxalate or phosphate ligands. The 2D sheets are interleaved by organic or inorganic cations. Because high coordination numbers (> six) are common for the lanthanoid metals, one can envisage a lanthanide oxalatophosphate with a covalently linked 3D honeycomb network structure. In addition, rare-earth complexes have been proved to have interesting luminescence properties and a wide range of applications.[4] Therefore, we have expanded our studies to the system of lanthanide/oxalate/phosphate or phosphite. Recently, we

* To whom correspondence should be addressed. E-mail: liikh@cc.ncu.edu.tw.
† Department of Chemistry, National Central University.
‡ Academia Sinica.
§ Department of Optics and Photonics, National Central University.

(1) (a) Cheetham, A. K.; Férey, G.; Loiseau, T. *Angew. Chem., Int. Ed.* **1999**, *38*, 3269. (b) Natarajan, S.; Mandal, S. *Angew. Chem., Int. Ed.* **2008**, *47*, 4798, and references therein.

10.1021/ic801817e CCC: $40.75
Published on Web 01/21/2009

reported the first examples of lanthanide oxalatophosphites $[Ln(H_2O)(C_2O_4)_{0.5}(HPO_3)]\cdot H_2O$ (Ln = Pr, Nd, Sm−Lu).[5] The structure of these 12 isostructural compounds consists of 2D layers of lanthanide phosphite, which are pillared through oxalate ligands to form a 3D framework. Following the successful synthesis of lanthanide oxalatophosphites, we report herein the first examples of organically templated lanthanide oxalatophosphates $(H_4APPIP)[Ln_2(C_2O_4)_{5.5}(H_2PO_4)_2]\cdot 5H_2O$ (Ln = Er−Lu, APPIP = 1,4-bis(3-aminopropyl)piperazine). These four compounds are isostructural and feature a 3D architecture in which 2D honeycomb layers of lanthanide oxalates are connected by dihydrogen phosphate and bis-monodentate oxalate ligands. The synthesis, structural characterization, thermal stability, variable-temperature in situ powder X-ray diffraction, guest desorption−sorption, magnetic susceptibility, luminescence, and catalytic properties are reported.

Experimental Section

Synthesis and Initial Characterization. Block crystals of $(H_4APPIP)Ln_3(C_2O_4)_{5.5}(H_2PO_4)_2\cdot 5H_2O$ (Ln = Er−Lu) were obtained by heating a mixture of $Ln(NO_3)_3\cdot xH_2O$ (0.25 mmol), H_3PO_4 (1.5 mmol), oxalic acid dihydrate (5.5 mmol), 1,4-bis(3-aminopropyl)piperazine (1 mmol), and H_2O (10 mL) in a Teflon-lined, 23 mL autoclave at 150 °C for 3 days. These four compounds are isostructural, as indicated by single-crystal and powder X-ray diffraction (see Figure S1 in the Supporting Information). The Er compound is pink, and the other three are colorless. Attempts to synthesize analogous compounds containing other lanthanoid metals were unsuccessful. Energy-dispersive X-ray fluorescence spectroscopic analysis of several crystals of $(H_4APPIP)[Er_3(C_2O_4)_{5.5}(H_2PO_4)_2]\cdot 5H_2O$ (denoted as **1**) confirms the presence of Er and P. Elemental analysis results of **1** are consistent with the formula [Anal. Found (Calcd): C, 17.02 (17.11); H, 3.01 (2.87); N, 3.84 (3.80)]. The IR spectrum was recorded on a BIO-RAD FT-IR spectrometer within the range of 400−4000 cm^{-1} using the KBr pellet method. Thermogravimetric analysis was performed on a powder sample in flowing O_2 within the temperature range from 40 to 900 °C by using a PerkinElmer TGA7 thermal analyzer. The guest desorption−sorption properties were investigated by using the same thermal analyzer. Variable-temperature in situ X-ray powder patterns were taken on a Siemens D5000 diffractometer.

Table 1. Crystallographic Data for $(H_4APPIP)Er_3(C_2O_4)_{5.5}(H_2PO_4)_2\cdot 5H_2O$

chemical formula	$C_{21}H_{42}Er_3N_4O_{35}P_2$
a/Å	8.5146(2)
b/Å	16.2049(5)
c/Å	28.5470(8)
β/°	96.212(2)
V/Å^3	3915.74(19)
Z	4
formula weight	1474.31
space group	$P2_1/c$ (No. 14)
T/°C	20
λ(Mo Kα)/Å	0.71073
D_{calc}/g·cm^{-3}	2.501
μ(Mo Kα)/cm^{-1}	65.79
R_1[a]	0.0327
wR_2[b]	0.0792

[a] $R_1 = \Sigma||F_o| - |F_c||/\Sigma|F_o|$. [b] $wR_2 = [\Sigma w(F_o^2 - F_c^2)^2/\Sigma w(F_o^2)^2]^{1/2}$, $w = 1/[\sigma^2(F_o^2) + (aP)^2 + bP]$, $P = [\mathrm{Max}(F_o,0) + 2(F_c)^2]/3$, where $a = 0$ and $b = 0.0292$.

Table 2. Selected Bond Lengths for $(H_4APPIP)Er_3(C_2O_4)_{5.5}(H_2PO_4)_2\cdot 5H_2O$

Er(1)−O(4)	2.289(4)	Er(1)−O(7)	2.332(3)
Er(1)−O(8)	2.390(4)	Er(1)−O(11)	2.405(4)
Er(1)−O(12)	2.326(3)	Er(1)−O(13)	2.467(4)
Er(1)−O(14)	2.392(4)	Er(1)−O(18)	2.265(4)
Er(2)−O(5)	2.367(4)	Er(2)−O(6)	2.382(3)
Er(2)−O(15)	2.430(4)	Er(2)−O(16)	2.360(4)
Er(2)−O(17)	2.256(4)	Er(2)−O(23)	2.317(3)
Er(2)−O(24)	2.416(4)	Er(2)−O(26)	2.286(4)
Er(3)−O(3)	2.229(4)	Er(3)−O(9)	2.385(3)
Er(3)−O(10)	2.350(4)	Er(3)−O(21)	2.348(4)
Er(3)−O(22)	2.349(3)	Er(3)−O(27)	2.310(4)
Er(3)−O(29)	2.434(4)	Er(3)−O(30)	2.426(4)
P(1)−O(1)	1.557(4)	P(1)−O(2)	1.590(4)
P(1)−O(3)	1.498(4)	P(1)−O(4)	1.501(4)
P(2)−O(17)	1.494(4)	P(2)−O(18)	1.483(4)
P(2)−O(19)	1.567(4)	P(2)−O(20)	1.592(4)

Single-Crystal X-ray Diffraction. A light pink crystal of dimensions 0.075 × 0.05 × 0.05 mm^3 of **1** was selected for indexing and intensity data collection on a Bruker APEX II X8 CCD diffractometer equipped with a normal focus, 3 kW sealed tube X-ray source. Intensity data were collected at room temperature in 1271 frames with ω scans (width 0.30° per frame). The SADABS program was used for the absorption correction ($T_{min/max} = 0.876/0.950$). On the basis of systematic absences and successful solution and refinement of the structure, the space group was determined to be $P2_1/c$ (No. 14). The structure was solved by direct methods and difference Fourier synthesis. Atom N(4) is disordered over two sites with equal occupancy. The H atoms bonded to C atoms in the organic amine molecule were positioned geometrically and refined using a riding model. Some of the other H atoms were located in difference Fourier maps. The H atoms of water molecules were not located. The final cycles of least-squares refinement including the atomic coordinates and anisotropic thermal parameters for all non-hydrogen atoms and fixed atomic coordinates and isotropic thermal parameters for the H atoms associated with the N atoms and H_2PO_4 groups converged at $R_1 = 0.0327$, $wR_2 = 0.0792$, and GOF = 1.048. The highest peak and deepest hole were 1.06 and −1.13 e/Å^3, respectively. All calculations were performed using SHELXTL, version 5.1, software package. Crystallographic data are listed in Table 1, and selected bond distances are reported in Table 2. Several crystals of **2**, **3**, and **4** were selected and indexed. Reflection profile analyses indicated that all crystals were twinned, and, therefore, their intensity data were not collected. Cell parameters for the Tm compound **2**: a = 8.4796(4) Å, b =

(2) (a) Lin, H.-M.; Lii, K.-H.; Jiang, Y.-C.; Wang, S.-L. *Chem. Mater.* **1999**, *11*, 519. (b) Lethbridge, Z. A. D.; Lightfoot, P. *J. Solid State Chem.* **1999**, *143*, 58. (c) Choudhury, A.; Natarajan, S.; Rao, C. N. R. *J. Solid State Chem.* **1999**, *146*, 538. (d) Do, J.; Bontchev, R. P.; Jacobson, A. J. *Chem. Mater.* **2001**, *13*, 2601. (e) Choi, C. T. S.; Anokhina, E. V.; Day, C. S.; Zhao, Y.; Taulelle, F.; Huguenard, C.; Gan, Z.; Lachgar, A. *Chem. Mater.* **2002**, *14*, 4096. (f) Jiang, Y.-C.; Wang, S.-L.; Lii, K.-H.; Nguyen, N.; Ducouret, A. *Chem. Mater.* **2003**, *15*, 1633. (g) Jiang, Y.-C.; Wang, S.-L.; Lee, S.-F.; Lii, K.-H. *Inorg. Chem.* **2003**, *42*, 6154. (h) Loiseau, T.; Férey, G.; Haousa, M.; Taullelle, F. *Chem. Mater.* **2004**, *16*, 5318. (i) Rao, C. N. R.; Natarajan, S.; Vaidhyanathan, R. *Angew. Chem., Int. Ed.* **2004**, *43*, 1466.

(3) (a) Tamaki, H.; Zhong, Z. J.; Matsumoto, N.; Kida, S.; Koikawa, M.; Achiwa, N.; Hashimoto, Y.; Okawa, H. *J. Am. Chem. Soc.* **1992**, *114*, 6974. (b) Mathonière, C.; Carling, S. G.; Yusheng, D.; Day, P. *J. Chem. Soc., Chem. Commun.* **1994**, 1551. (c) Decurtins, S.; Schmalle, H. W.; Oswald, H. R.; Linden, A.; Ensling, J.; Gütlich, P.; Hauser, A. *Inorg. Chim. Acta* **1994**, *216*, 65. (d) Day, P. *J. Chem. Soc., Dalton Trans.* **1997**, 701. (e) Decurtins, S.; Pellaux, R.; Antorrena, G.; Palacio, F. *Coord. Chem. Rev.* **1999**, *841*, 190–192, and references therein.

(4) (a) Richardson, F. S. *Chem. Rev.* **1982**, *82*, 541. (b) McGehee, M. D.; Bergstedt, T.; Zhang, C.; Saab, A. P.; O'Regan, M. B.; Bazan, G. C.; Srdanov, V. I.; Heeger, A. J. *Adv. Mater.* **1999**, *11*, 1349. (c) Kido, J.; Okamoto, Y. *Chem. Rev.* **2002**, *102*, 2357. (d) Kuriki, K.; Koike, Y. *Chem. Rev.* **2002**, *102*, 2347.

(5) Wang, C.-M.; Wu, Y.-Y.; Chang, Y.-W.; Lii, K.-H. *Chem. Mater.* **2008**, *20*, 2857.

16.1414(6) Å, c = 28.3534(9) Å, β = 96.292(3)°. The Yb compound **3**: a = 8.4674(3) Å, b = 16.1367(6) Å, c = 28.161(1) Å, β = 96.568(3)°. The Lu compound **4**: a = 8.4513(9) Å, b = 16.108(2) Å, c = 28.254(2) Å, β = 96.219(6)°.

Physical Measurements. The near-IR luminescence spectra of **1** were measured in the wavelength range of 1400−1700 nm using a 980 nm laser diode as the excitation source and an InGaAs detector. The as-synthesized solid of **1** for the PL measurements was prepared by pressing a powder sample into a thin plate sandwiched between two glass slides. To study the luminescence properties of the dehydrated compound of **1**, the dehydrated sample was prepared by heating a thin plate of **1** at 200 °C for 1 h and then sealed between two glass slides. The near-IR luminescence spectrum of **3** was measured using an Edinburgh FL920 fluorescence spectrometer. Variable-temperature magnetic susceptibilities were measured on a 29.6 mg powder sample of **1** using a SQUID system between 2 and 300 K in a magnetic field of 0.2 T. Susceptibility values were corrected for the sample diamagnetic contribution (−501 × 10^{-6} emu/formula unit).

Catalytic Properties. The Yb compound was chosen as a catalyst for the Biginelli reaction. Initially, a mixture of benzaldehyde (0.5 mmol), ethylacetoacetate (0.5 mmol), urea (0.6 mmol), a powder sample of **3** (0.05 mmol), and methanol (2 mL) was stirred in a 20 mL glass vial at rt for 48 h, then 5 mL of water was added, and the product was extracted with ethyl acetate (3 × 5 mL). The organic layer was dried with anhydrous $MgSO_4$ and evaporated, and then the residue was purified by prepared TLC (ether/ethyl acetate = 3:1) to afford 5-ethoxycarbonyl-6-methyl-4-phenyl-3,4-dihydropyrimidin-2(1*H*)-one, which was characterized by ^{1}H NMR and fast atom bombardment (FAB) mass spectrometry. The used catalyst was collected by filtering the water layer, washed with water, rinsed with ethanol, and dried in a desiccator, and it can be reused for the study of catalytic activity.

Results and Discussion

Characterization. The infrared spectrum of **1** reveals the bands characteristic of an O−H stretch (∼3500 cm^{-1}), the organic molecule (3150, 3030 cm^{-1}), oxalate ligand (1640 cm^{-1}), and phosphate group (1160, 1080, 970 cm^{-1}) (Figure S2 in the Supporting Information). Thermogravimetric analysis measurements in flowing O_2 at 5 °C min^{-1} from 40 to 800 °C and at 1 °C min^{-1} from 800 to 900 °C showed a weight loss in several overlapping steps (Figure 1a). The weight loss of 5.85% between 40 and 250 °C confirms the presence of five lattice water molecules (6.11%). The observed total weight loss of 49.24% between 40 and 900 °C is close to the calculated value of 49.28% for the loss of one APPIP, 5.5 CO_2, 5.5 CO, and nine H_2O molecules. To study guest desorption−sorption properties, a dehydrated Er compound was exposed to moist air at room temperature for 1 day and then was heated to 200 °C at 5 °C min^{-1} by using the same thermal analyzer. The results show that the dehydrated compound can absorb water reversibly (Figure 1b). The dehydration and hydration process has also been studied by variable-temperature in situ powder X-ray diffraction. The pattern for dehydration at 200 °C shows that the sample remains crystalline but with a crystallographic modification and that re-adsorption by exposing it to air at ambient temperature for 1 day confirms that the integrity of the framework is not affected by the release of water molecules (Figure 2). Attempts to determine the crystal

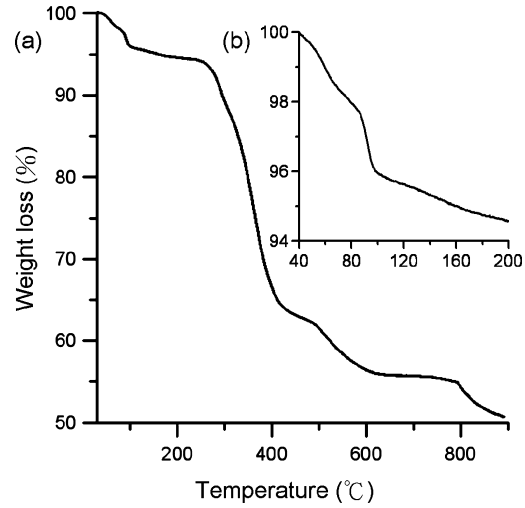

Figure 1. (a) Thermogravimetric analysis of **1** in flowing air at 5 °C min^{-1} from 40 to 800 °C and at 1 °C min^{-1} from 800 to 900 °C. (b) Dehydrated Er compound after exposing it to moist air for 1 day was heated at 5 °C min^{-1} from 40 to 200 °C.

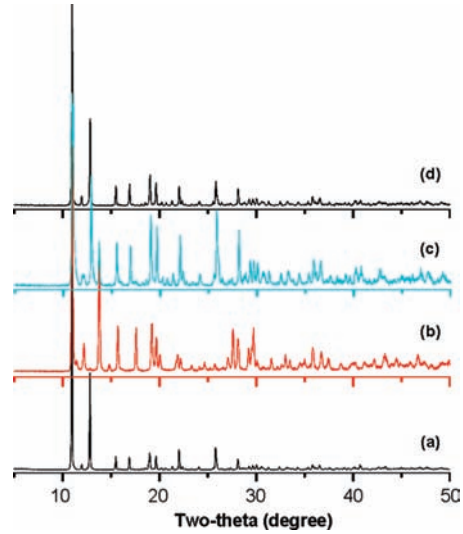

Figure 2. Variable-temperature in situ PXRD for **1**: (a) as-synthesized, (b) holding at 200 °C for 1 h, (c) after cooling to room temperature, and (d) exposed to air at room temperature for 1 day.

structure of the dehydrated Er compound by single-crystal X-ray diffraction were unsuccessful because of the poor crystal quality of the dehydrated crystals.

Structure. As revealed by single-crystal X-ray crystallography, the structure of **1** is constructed from the following structural elements: one $(H_4APPIP)^{4+}$ cation, three distinct ErO_8 polyhedra, six $C_2O_4^{2-}$ ligands, two $H_2PO_4^-$ groups, and five lattice water molecules. The coordination environments of the Er^{3+} cations and atom labeling scheme are shown in Figure 3. The Er^{3+} cations are eight-fold coordinated by oxygen atoms in a geometry of trigonal dodecahedron, which is a common structure for eight-coordination. Er(1) is coordinated by three bis-bidentate $C_2O_4^{2-}$ and two $H_2PO_4^-$ ligands, whereas Er(2) and Er(3) are coordinated by three bis-bidentate $C_2O_4^{2-}$, one bis-monobidentae $C_2O_4^{2-}$, and one $H_2PO_4^-$ ligand. All oxalate units except $C(9)C(10)O_4$ show only bis-bidentate coordination to two Er^{3+} ions. One of the five bis-bidentate oxalates, $C(11)_2O_4$, sits on an inversion

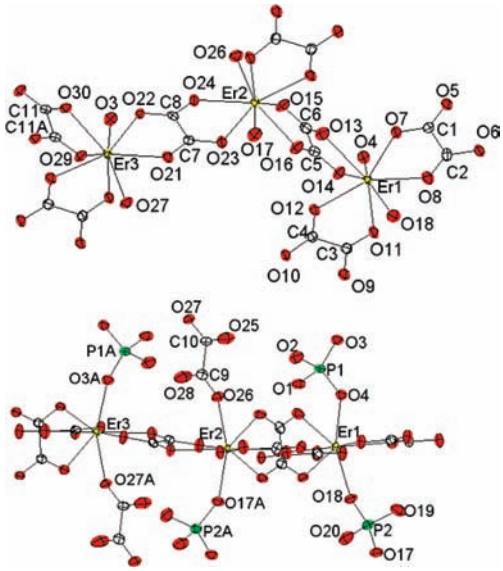

Figure 3. Coordination environments of the Er^{3+} ions in the structure of **1** showing atom labeling scheme. Thermal ellipsoids are shown at 50% probability.

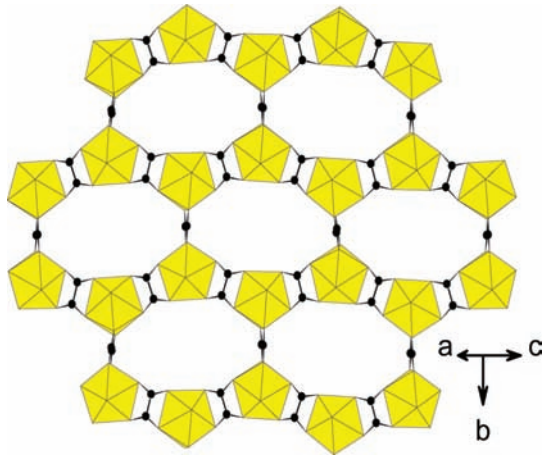

Figure 4. Section of a layer of Er oxalate in **1** viewed in a direction perpendicular to the (102) plane.

center and is coordinated to two $Er(3)^{3+}$ ions. The $C(9)C(10)O_4$ unit is a bis-monodentate ligand to Er(2) and Er(3) in trans orientation, which is an unusual coordination mode.[6]

As shown in Figure 4, each ErO_8 trigonal dodecahedron is linked by three bis-bidentate oxalates to form layers in the (102) plane, which are connected by bis-monodentate oxalate and phosphate ligands to form a 3D framework. The 12-membered ring straight channels along the *a* axis are formed by the edges of six ErO_8 trigonal dodecahedra, three $C_2O_4^{2-}$, and three $H_2PO_4^-$ units, in which tetraprotonated 1,4-bis(3-aminopropyl)piperazinium cations and lattice water molecules reside (Figure 5). The water molecules form extensive hydrogen bonds with framework oxygen atoms, the organic cations, and neighboring water molecules, as indicated by short Ow···O, Ow···N, and Ow···Ow distances (Ow(1)···O(4), 2.914 Å; Ow(2)···O(8), 2.940 Å; Ow(3)···O(22), 2.900 Å; Ow(1)···N(1), 2.960 Å; Ow(2)···N(1), 2.855 Å; Ow(1)···Ow(4), 2.933 Å; Ow(3)···Ow(4), 3.061 Å; Ow(5)···Ow(5), 2.553 Å).

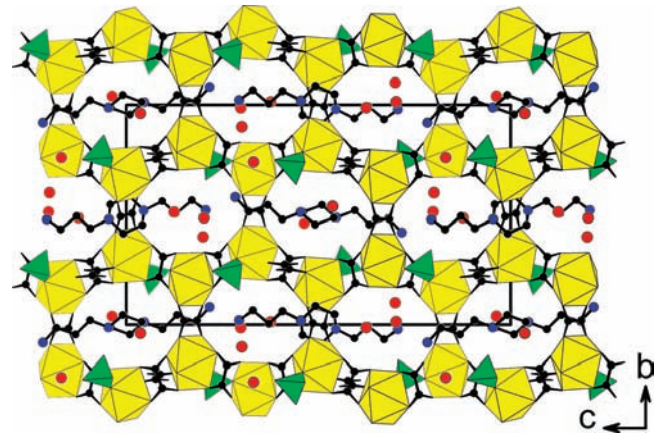

Figure 5. Structure of **1** viewed along the *a* axis. The yellow and green polyhedra are ErO_8 trigonal dodecahedra and H_2PO_4 tetrahedra, respectively. Black circles, C atoms; blue circles, N atoms; red circles, water oxygen atoms. H atoms are not shown for clarity.

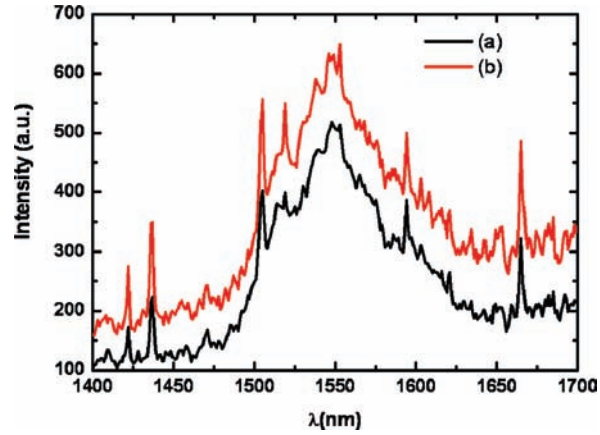

Figure 6. Luminescence spectrum of **1** excited at 980 nm: (a) as-synthesized and (b) dehydrated.

A few organically templated metal oxalates with a 3D honeycomb structure have been reported.[2i] They are all built of bis-bidentate linkages between the metal and oxalate ligands, forming layers with 12-membered, honeycomb-like apertures pillared to open-framework architectures by another bis-bidentate oxalate. For example, the 3D honeycomb structures of the two yttrium oxalates, $[C_6N_2H_{16}]_{0.5}[Y(H_2O)(C_2O_4)_2]\cdot 2H_2O$ and $[C_5N_2H_{12}][Y(C_2O_4)_2]$, are formed by Y and the bis-bidentate oxalate ligands.[7] However, in our case, these bis-bidentate linkers in lanthanide oxalates are replaced by bis-monodentate oxalate and dihydrogen phosphate ligands to form a new family of rare-earth compounds.

Luminescence Properties. Figure 6 shows the room temperature near-IR photoluminescence spectra of the as-synthesized and the dehydrated Er compounds, which were recorded from 1400 to 1700 nm using a 980 nm excitation source. The spectra display a broad emission at about 1550 nm that can be attributed to the $^4I_{13/2} \rightarrow {}^4I_{15/2}$ transition for the Stark splitting of degenerate 4f energy levels of the Er^{3+}

(6) (a) Vaidhyanathan, R.; Natarajan, S.; Rao, C. N. O. *Mater. Res. Bull.* **2003**, *38*, 477. (b) Park, H.; Kim, J. C.; Lough, A. J.; Lee, B. M. *Inorg. Chem. Commun.* **2007**, *10*, 303.

(7) Vaidhyanathan, R.; Natarajan, S.; Rao, C. N. R. *Chem. Mater.* **2001**, *13*, 185.

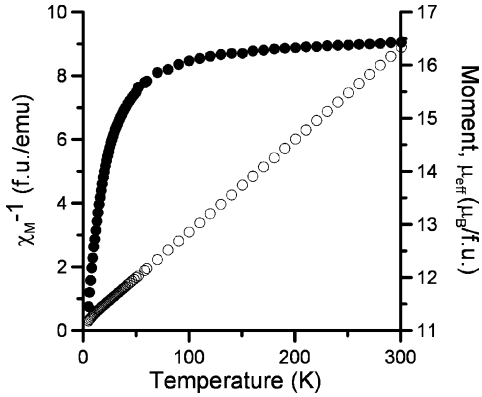

Figure 7. μ_{eff} versus T (●) and $1/\chi_M$ versus T (○) for **1**.

ion. The spectra are analogous to the previously reported spectrum of erbium−organic frameworks.[8] The spectral intensity of the as-synthesized Er compound is lower than that of the dehydrated one, which can be attributed to the reduction of the quenching effect of water molecules.[9] The Yb compound displays a broad emission at about 1080 nm (Figure S3 in the Supporting Information) that can be attributed to the $^2F_{5/2} \rightarrow {}^2F_{7/2}$ transition for the Yb^{3+} ion.[10]

Magnetic Susceptibility. The temperature dependence of μ_{eff} and χ_M^{-1} curves is shown in Figure 7. The effective magnetic moment at 300 K is 16.44 μ_B/per formula as compared to the theoretical value of 16.58 μ_B for three Er^{3+} ions per formula. The magnetic moment decreases rapidly upon cooling, which indicates the presence of antiferromagnetic interactions between the Er^{3+} ions. A fit of the data from the equation $\chi_M = C/(T - \theta)$ results in $C = 34.64$ $cm^3 \cdot K/mol$ and $\theta = -7.73$ K. The effective magnetic moment obtained using $\mu_{eff} = [8(C/3)]^{1/2}$ is 9.61 μ_B/Er^{3+}, which is close to the value (9.57 μ_B) calculated by the equation $\mu_{eff} = g_J[J(J + 1)]^{1/2}$ ($g_J = 6/5$, $J = 15/2$).

Catalyzed Biginelli Reaction. Many useful reactions in organic synthesis are catalyzed by rare-earth-metal compounds.[11] Among those interesting transformations, the Biginelli reaction is a good way to synthesize many dihydropyrimidinones and their derivatives, which are important for pharmacological research. Recently, lanthanide compounds such as $Yb(OTf)_3$, Gd-notp, and $[Gd(H_2O)(C_2O_4)_{0.5}(HPO_3)] \cdot H_2O$ were reported to be effective catalysts for the Biginelli reaction.[5,12] Therefore, we explored the Biginelli reaction by using $(H_4APPIP)[Yb_3(C_2O_4)_{5.5}(H_2PO_4)_2] \cdot 5H_2O$ (**3**) as a catalyst. After the catalytic reaction was carried out, 5-ethoxycarbonyl-6-methyl-4-phenyl-3,4-dihydropyrimidin-2(1*H*)-one was isolated by a TLC method. The yield (25%) is considerably lower than those when $Yb(OTf)_3$ and its derivatives are used as catalysts. Because the resultant organic molecule is too large to be accommodated within pores, the catalytic reaction could be a simple surface reaction. No product was obtained in the absence of compound **3**. Besides, the catalyst can be reused for this reaction, and the yield is 27%, indicating no loss of catalytic activity. The product was characterized by ^1H NMR and fast atom bombardment (FAB) mass spectrometry. ^1H NMR (Figure S4 in the Supporting Information, 300 MHz, DMSO, TMS): δ 9.20 (s, 1H, NH), 7.75 (s, 1H, NH), 7.35−7.29 (m, 2H, Ar−H), 7.26−7.22 (m, 3H, Ar−H), 5.15 (s, 1H, CH), 4.01−3.94 (q, J = 7.2 Hz, 2H, $-OCH_2-$), 2.24 (s, 3H, $-CH_3$), 1.11−1.06 ppm (t, J = 7.2 Hz, 3H, $-CH_3$). FAB-MS: $m/z = 261.1$ $[M + H]^+$.

In conclusion, we have synthesized the first organically templated lanthanide oxalatophosphates by a hydrothermal method. Their structures consist of 2D layers of lanthanide oxalates, which are connected by bis-monodentate oxalate and dihydrogen phosphate ligands to generate a 3D open framework. The Er and Yb compounds show near-infrared luminescence at about 1550 and 1080 nm, respectively. The study on the catalytic properties of the Yb compound shows that it can be a catalyst for the Biginelli reaction. Previously, we reported two transition-metal oxalatophosphates with a 2D honeycomb structure.[2g] The higher coordination numbers and various stereochemistries of the lanthanides facilitate the formation of a 3D honeycomb network structure, as observed in the title compounds. Other possible 3D architectures can be envisaged. For example, we have recently synthesized a novel lanthanide phosphate framework by using a new organic linker, which will be published elsewhere. The scope for research in this area with regard to the synthesis of 3D frameworks with new topologies appears to be very large.

Acknowledgment. We thank the National Science Council for support, and Dr. Y.-S. Wen at the Institute of Chemistry, Academia Sinica, for X-ray data collection.

Supporting Information Available: Crystallographic data, room temperature X-ray powder patterns, infrared spectrum, and ^1H NMR spectra. This material is available free of charge via the Internet at http://pubs.acs.org.

IC801817E

(8) Chen, B.; Yang, Y.; Zapata, F.; Qian, G.; Luo, Y.; Zhang, J.; Lobkovsky, E. B. *Inorg. Chem.* **2006**, *45*, 8882.
(9) Song, J.-L.; Mao, J.-G. *Chem.—Eur. J.* **2005**, *11*, 1417.
(10) Feng, M.-L.; Mao, J.-G. *Eur. J. Inorg. Chem.* **2007**, 5447.
(11) Kobayashi, S.; Sugiura, M.; Kitagawa, H.; Lam, W. W.-L. *Chem. Rev.* **2002**, *102*, 2227.
(12) (a) Kappe, C. O. *Acc. Chem. Res.* **2000**, *33*, 879. (b) Lusch, M. J.; Tallarico, J. A. *Org. Lett.* **2004**, *6*, 3237. (c) Ma, Y.; Qian, C.; Wang, L.; Yang, M. *J. Org. Chem.* **2000**, *65*, 3864. (d) Huang, Y.-H.; Yang, F.; Zhu, C. *J. Am. Chem. Soc.* **2005**, *127*, 16386. (e) Bao, S.-S.; Ma, L.-F.; Wang, Y.; Fang, L.; Zhu, C.-J.; Li, Y.-Z.; Zheng, L.-M. *Chem.—Eur. J.* **2007**, *13*, 2333.